COSMIC RAY GROUP

School of Physics and Astronomy

UNIVERSITY OF MINNESOTA

Description of Data Plots from the University of Minnesota Ion Chamber and Electron Spectrometer on OGO-I and OGO-III

This report and the OGO data analysis prepared by:

S. R. Kane, K. A. Pfitzer and J. R. Winckler

CR-127

February, 1969

School of Physics and Astronomy
University of Minnesota
Minneapolis, Minnesota

This work has been supported by the National Aeronautics and Space Administration under Contract NAS 5-2071 and Grant NGR-24-005-008.

TABLE OF CONTENTS

I. Introduction and General Description

This report is intended to explain and clarify the extensive series of Cal-Comp computer produced plots of the two University of Minnesota experiments flown on the OGO-I and OGO-III satellites. A description has already been prepared of the instruments and how the output data is produced and handled by the satellite as follows:

Kane, S. R., K. A. Pfitzer and J. R. Winckler, The Construction, Calibration and Operation of the University of Minnesota Experiments for OGO-I and OGO-III, University of Minnesota Cosmic Ray Technical Report No. CR-87, September, 1966.

Kane, S. R., Application of an Integrating Type Ionization Chamber to Measurements of Radiation in Space, Ph.D. Thesis, University of Minnesota Cosmic Ray Technical Report No. CR-106, September, 1967.

Pfitzer, K. A., An Experimental Study of Electron Fluxes from 50 keV to 4 meV in the Inner Radiation Belt, Ph.D. Thesis, University of Minnesota Cosmic Ray Technical Report No. CR-123, August, 1968.

The various formats devised for these data plots have been arranged to exploit the data for various uses as the need arose. Thus, the plots give ionization rate, for example, on linear and logarithmic scales plotted as a function of distance, time, L-value, etc. and similarly for the electron spectrometer. In the case of the ionization chamber, the instrument is sensitive to a wide variety of types of radiations and all of these types may be seen singly or superposed in the data. Thus, suitable discrimination must be used in the interpretation. The reader is referred to bibliographies of published papers under the OGO program for detailed examples of this as well as in the above three listed references. In the case of the electron spectrometer it is a highly selective instrument responding only to electrons in the radiation belt regions, but much complexity arises because of the aspect or view angle of the instrument and its rapid passage through different particle shells and different latitudes and radial distance. Thus, the spectrometer rates are plotted against time, distance, L-values, etc. In addition, orbital information giving the pitch angles sampled, etc. are included on separate graphs. The calibration factors for determining the electron flux and energy spectra from the spectrometer arbitrary rate scales are included in Section III. In the case of the ionization chamber the normalized pulsing rate is given on the graphs. Conversion of this to absolute fluxes of given radiation type may be done by reference to the above three reports.

The basic plots are of the following type:

Type	Spectrometer	Ion Chamber
1. Rate vs. time		
Log scale ($L \leq 3$)	X	X
Log scale ($L \leq 15$)	X	X
Log scale (All L)		X
Linear scale (All L)		X
Linear scale (hourly averages)		X
2. Rate vs. distance R		
Log scale ($R \leq 23$) OGO-A	X	X
Log scale ($R \leq 18$) OGO-B	X	X
3. Rate vs. L		
Log scale ($L \leq 8$)	X	X
4. Orbital Parameters		
α_0, α_B, ϕ, L vs. R ($R \leq 23$)		
α_0, α_B, ϕ vs. L ($L \leq 8$)		

Special plots for certain data are as follows:

Type	Spectrometer	Ion Chamber
1. Rate vs. day		
Outside magnetosphere (daily mean rate)		X
Outer zone (L = 4, 5, 6, 7)	X	X
Inner zone - corrected for latitude (L = 1.3, 1.4, 1.5, 1.6, 1.7, 1.8, 1.9, 2.0, 2.2, 2.4, 2.6, 3.0)	X	X
2. Rate vs. pitch angle		
Inner zone (L = 1.3, 1.4, 1.5, 1.6, 1.7, 1.8, 1.9, 2.0, 2.2, 2.4, 2.6, 3.0)	X	X

II. Sample Data Plots with Explanations

Explanation of "Plot Type"

Format: L' L" - L"'

where L', L" and L"' are letters.

Significance:

L' represents the name of the instrument:

C for ion chamber

E for electron spectrometer

D for orbit of the satellite

L" represents the type of plot (parameters plotted, scales and symbols used, etc.). The letters vary from A to F and their significance may vary from one instrument to the other.

L"' represents the name of the satellite:

A for OGO-I

B for OGO-III

Example: Plot type CB-A

This represents OGO-I ion chamber data plot of type B.

Explanation of Plot Number

Each data plot is numbered in the format:

L' L" - L"' - N' N" N"'

where L', L", L"' are letters and represent the Plot Type.

N', N", N"' are numerals constituting the serial number of the plot.

Example: CB-A-159

This represents the 159th plot belonging to the Plot Type CB-A, i.e., plot B of the OGO-I ion chamber data.

Electron Spectrometer Data Plots

The electron spectrometer data are plotted against time, range and L. All of the spectrometer rates are plotted in the same arbitrary scale which must be multiplied by the correction factors to obtain the electron fluxes or the differential energy spectra. See Section III for a description of the procedure.

The data for the five energy channels are background corrected and plotted with the statistical error bars. Only a limited amount of noise filtering has been performed and hence some caution must be exercised when using the plots. Figures 1 through 6 give examples of the types of spectrometer plots available. Each figure is completely described by the figure caption.

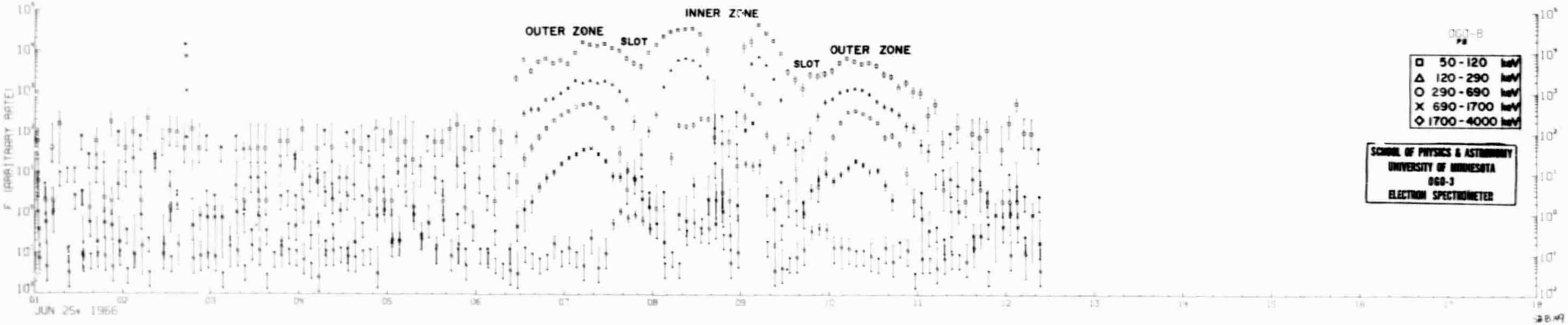

Figure 1

5 minute averages of the spectrometer rate plotted vs. time. The total time covered by the plot is one third of an orbit with perigee at the center of the plot. Since this plot is an OGO-III plot between June 9, 1966 and July 25, 1966, the playback and real time data are plotted on separate graphs. This plot is from playback data as indicated by the small "PB" in the upper right hand corner.

The radiation belt electron fluxes are clearly evident above the statistical background fluctuations seen outside the radiation belts. (Figure 5 will describe in detail a pass through the radiation belts.)

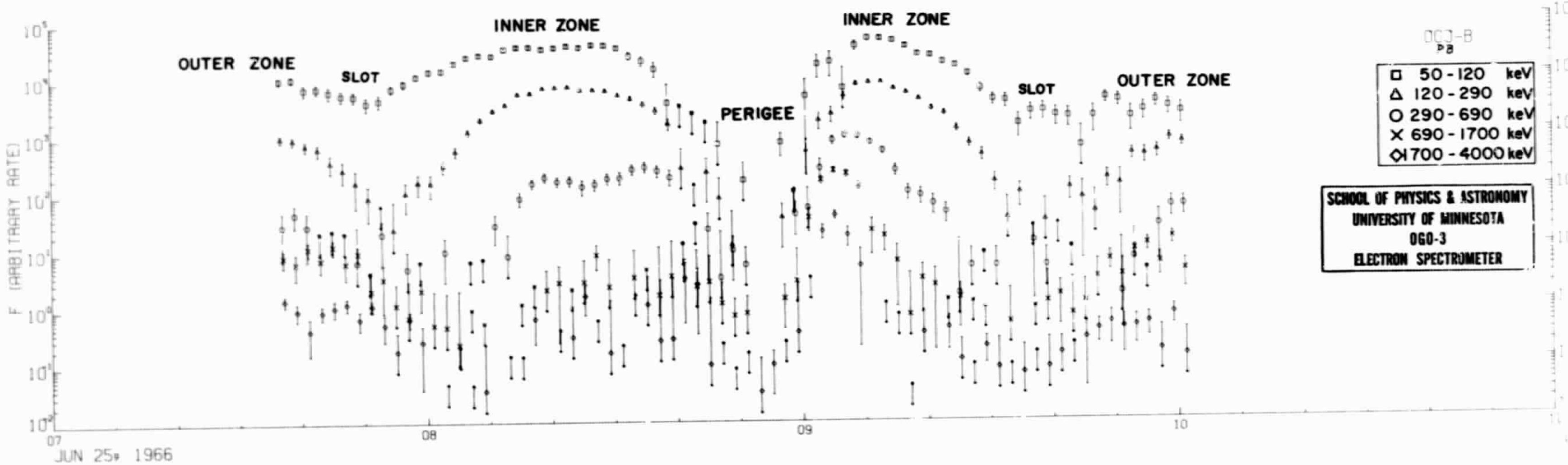

Figure 2

This plot represents an expanded view of the inner zone for $R_e \leq 3$ for the same data covered in Figure 1. Two minute averages are plotted versus time.

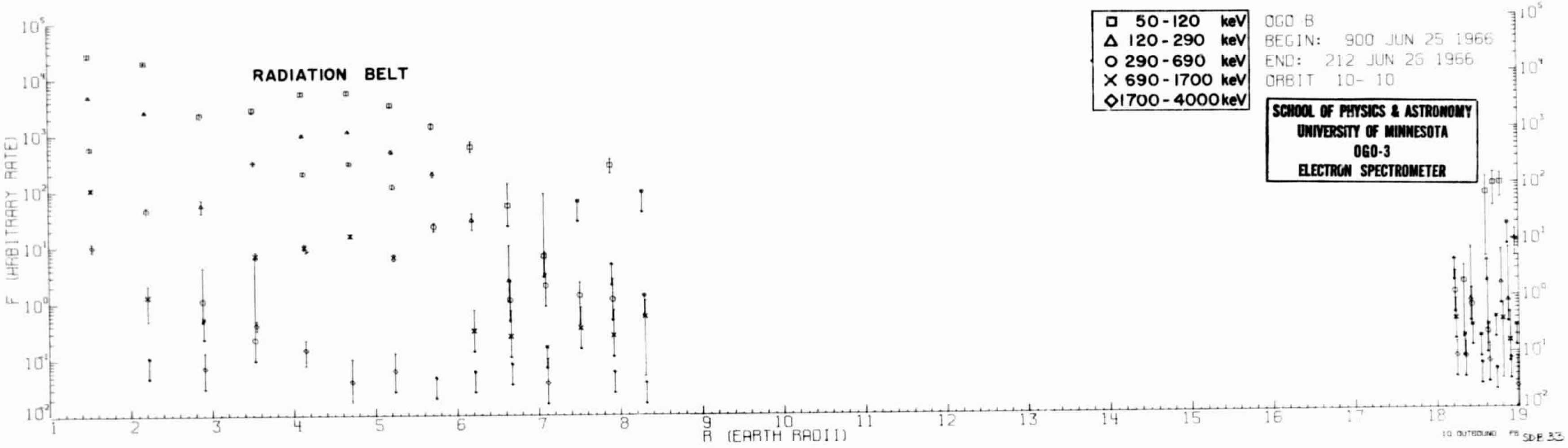

Figure 3

A portion of the pass shown in Figures 1 and 2 is plotted in Figure 3 vs. range using 15 minute averages. The plot represents playback data only, and the real time data for this pass is shown in the next figure (Figure 4). The symbol "PB" is located in the lower right hand corner indicating the playback data. The word "OUTBOUND" in the lower left hand corner indicates that the data starts at perigee and ends at apogee. "INBOUND" is written when referring to pass beginning at apogee and ending at perigee. The begin and end times in the upper right hand corner represent the begin and end times of the plot and not necessarily of the data.

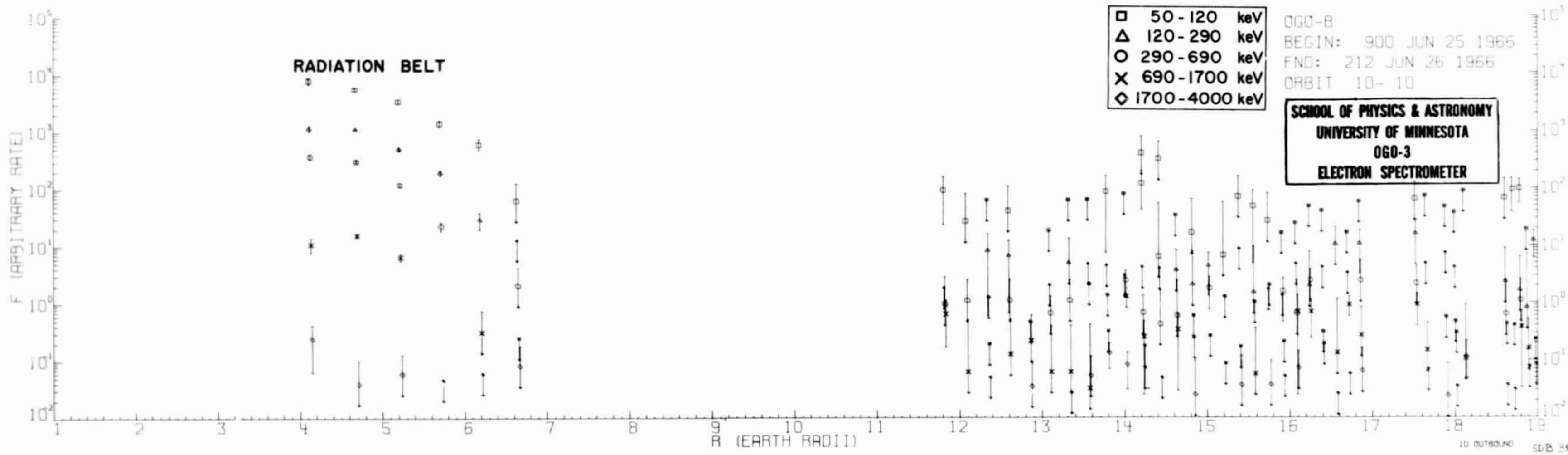

Figure 4

This plot is the same as Figure 3 except that this is a plot of the real time data. The real time and playback data usually supplement each other, but they also overlap in many instances.

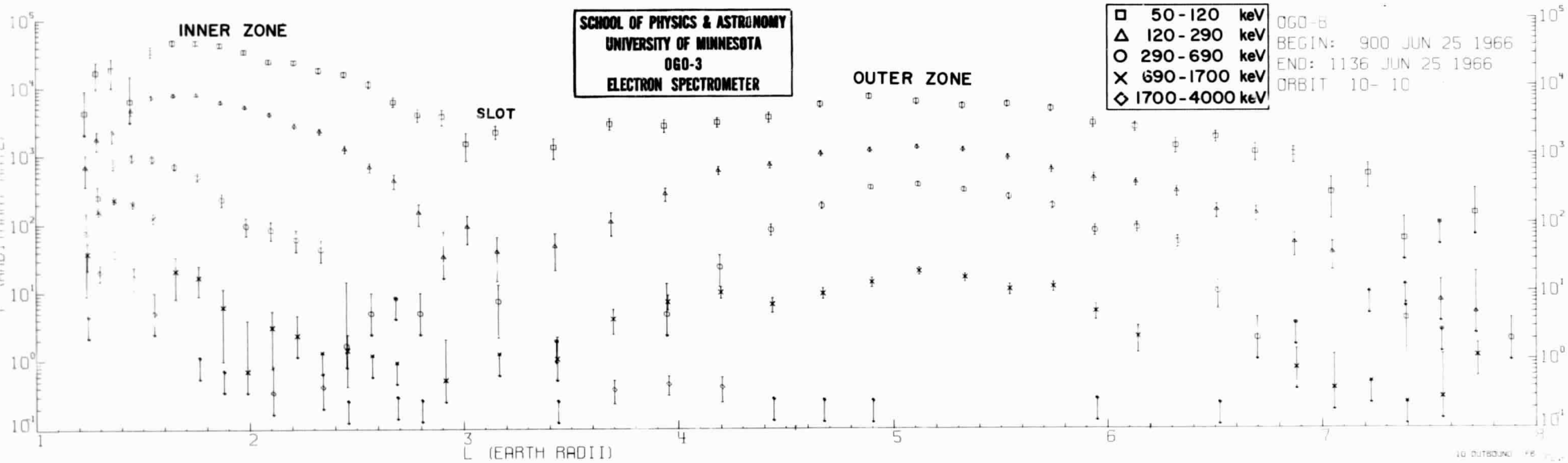

Figure 5

An example of an electron spectrometer pass through the radiation belts showing the five energy channels plotted versus L. For L $\leq$ 3 two minute averages are plotted; for L $\geq$ 3 five minute averages are plotted.

The plot begins at perigee, where the fluxes are low due to atmospheric attenuation and then passes through the heart of the inner zone into the slot. The slot between the belts is characterized by high loss rates (typical of the outer zone) and by low injection rates (typical of the inner zone). The slot is most pronounced for high energies and often ceases to exist at E < 690 keV following large magnetic storms. The peak in the outer zone is also clearly evident.

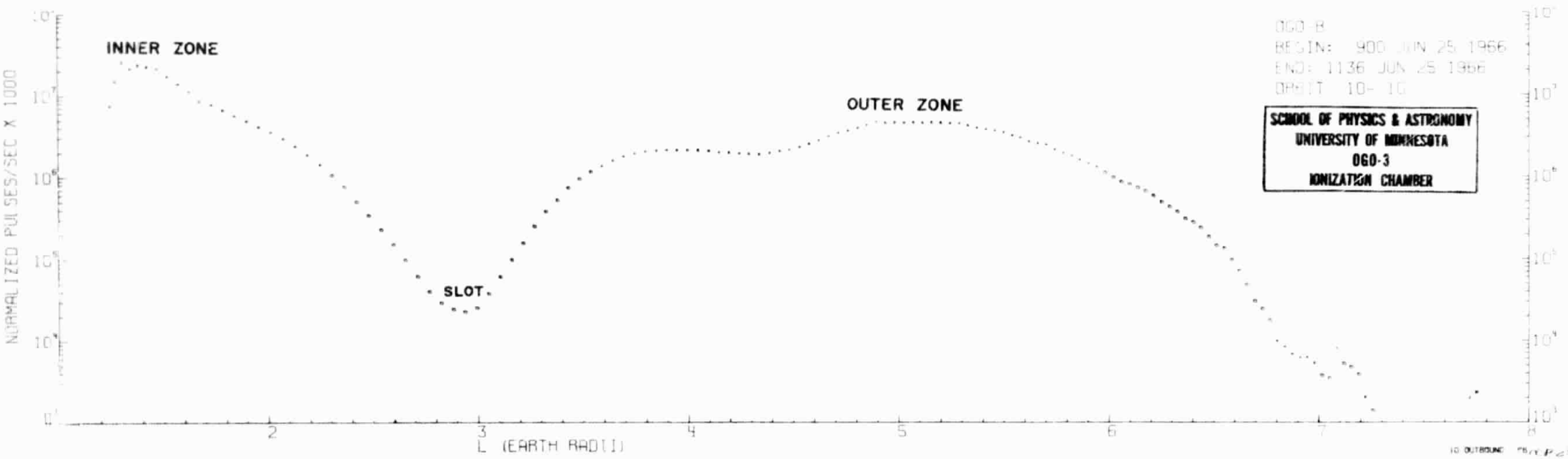

Figure 6

An example of an ion chamber pass covering the same data as the spectrometer pass in Figure 5. The ion chamber is sensitive to electrons above 600 keV and hence one can note the excellent agreement of the ion chamber with the 690-1700 keV spectrometer channel. Since the threshold sensitivity of the ion chamber is much lower than the spectrometer the ion chamber data can be used to extend the range of the electron measurement in the 600 keV range.

The ion chamber exhibits a very deep slot at L = 3. In the outer zone the ion chamber responds primarily to electrons; whereas, in the inner zone the ion chamber responds primarily to protons.

Ion Chamber Plots

All ion chamber data are plotted against a normalized scale. A complete description and calibration is available in Kane (1967) and Kane et al. (1966) (see references, page 1). Some chamber data are plotted in a histogram fashion; whereas in other cases symbols represent each data point. The histogram is filtered and if the filter fails a symbol is used to represent the "spurious" data point. Since the chamber transmits a given piece of information in three separate ways the type of symbol used represents the amount of agreement between methods of transmission and filtering. The symbols are explained in the following table:

Symbols used on ion chamber plots to indicate data quality may be as follows:

	Symbol
Unfiltered word 43 (resets)	A
Filtered word 43 (resets)	B
Clock pulses	C
C, A agreement (within 10%)	+
B, A agreement (within 10%) (c=0)	⌧
C, B agreement (within 10%)	Θ
B, A agreement (within 10%) ($c \neq 0$)	*
C no agreement even though A, B present	X

Further symbols on certain plots are the following:

R = geocentric distance in earth radii	◈
ϕ = local time in degrees (midnight = 0°)	▲
α_0 = equatorial pitch angle (used for spectrometer)	X
α_B = maximum equatorial pitch angle (used for ion chamber	Θ

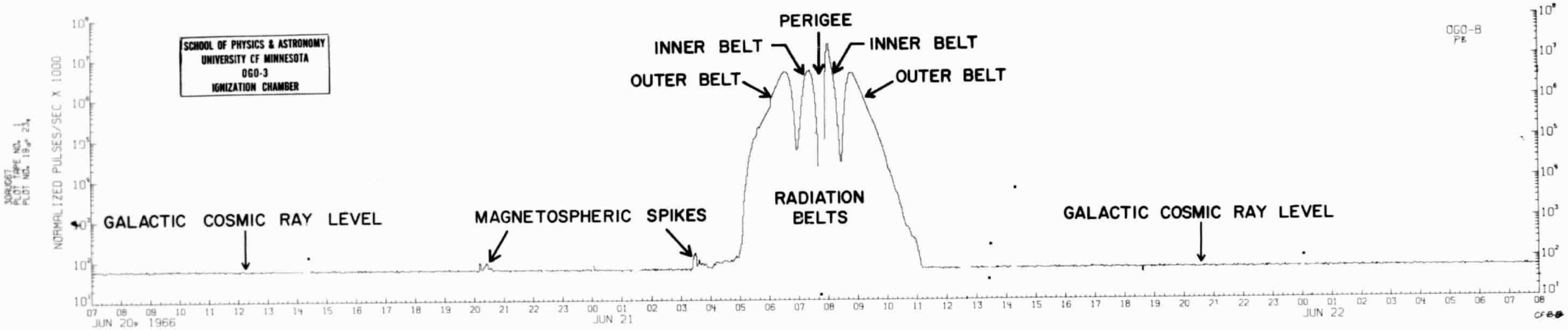

Figure 7

This figure shows a complete apogee to apogee orbit for the ion chamber. Two-minute averages are plotted versus time. The various phenomena encountered by the chamber during this typical pass are clearly indicated by the labels.

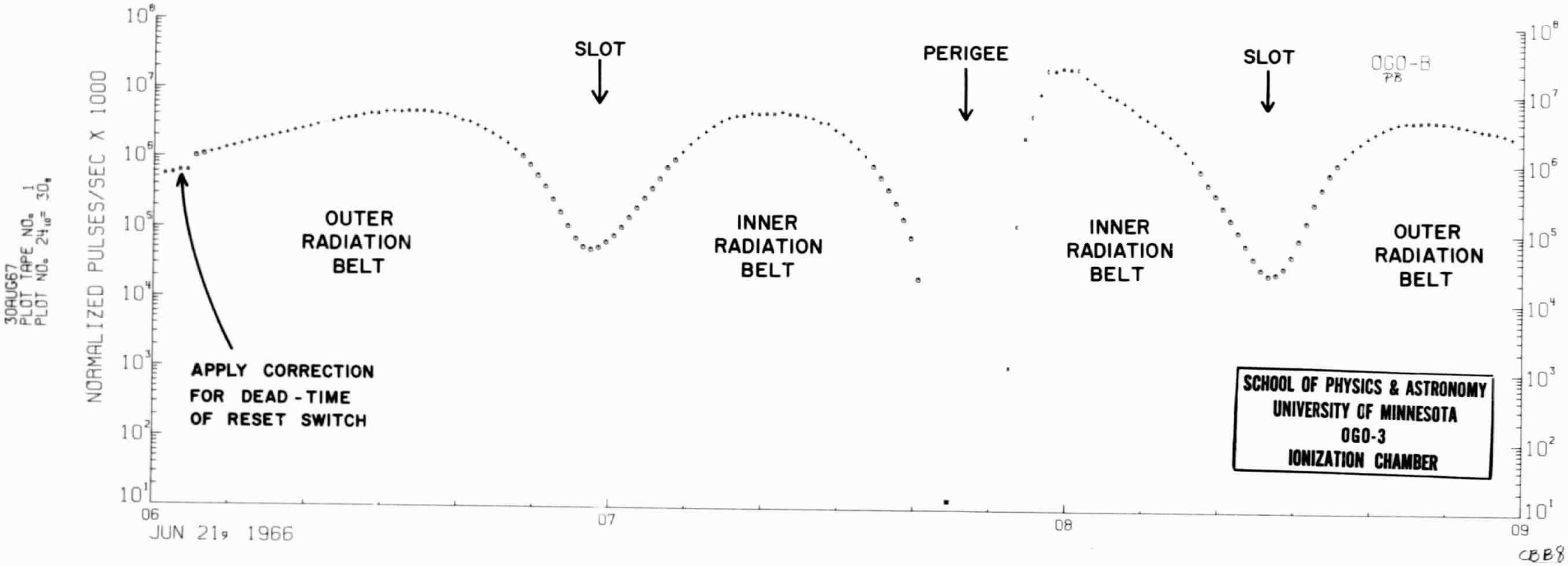

Figure 8

An expanded time plot consisting of one-minute averages for the region near perigee ($R_e \leq 3$). One can note the inner edge of the outer zone, the slot, the inner zone and the dip below the radiation belts. The data point at perigee is a factor of about 3 below galactic cosmic ray levels.

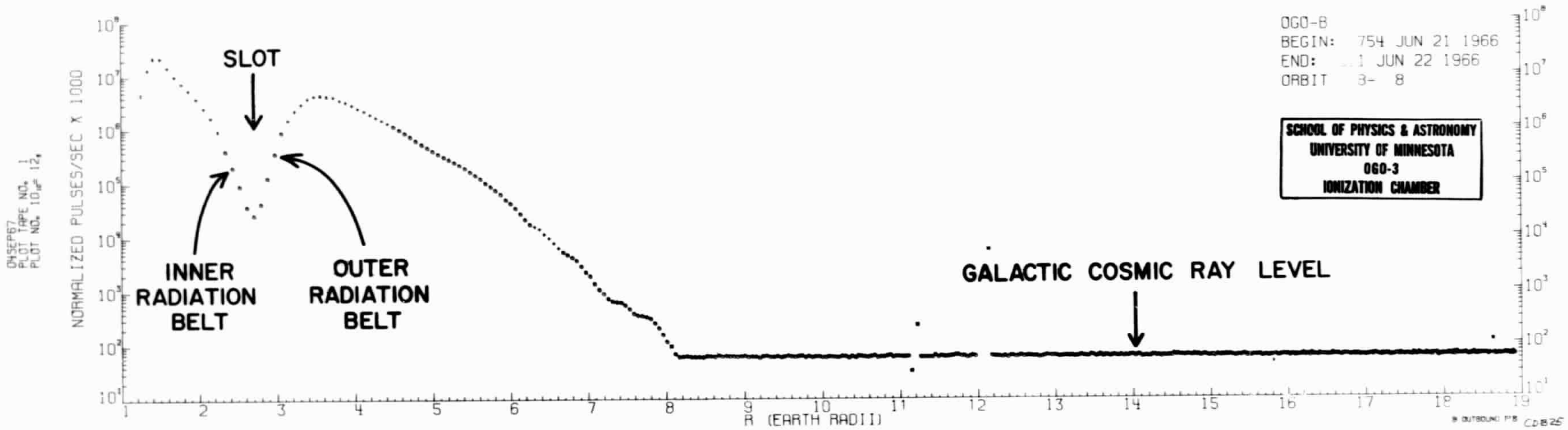

Figure 9

The figure represents a perigee to apogee pass plotted versus range. This plot represents playback data only as indicated by the "PB" in the lower right hand corner. The beginning and ending times of the plot (not necessarily of the data) are given in the upper right hand corner.

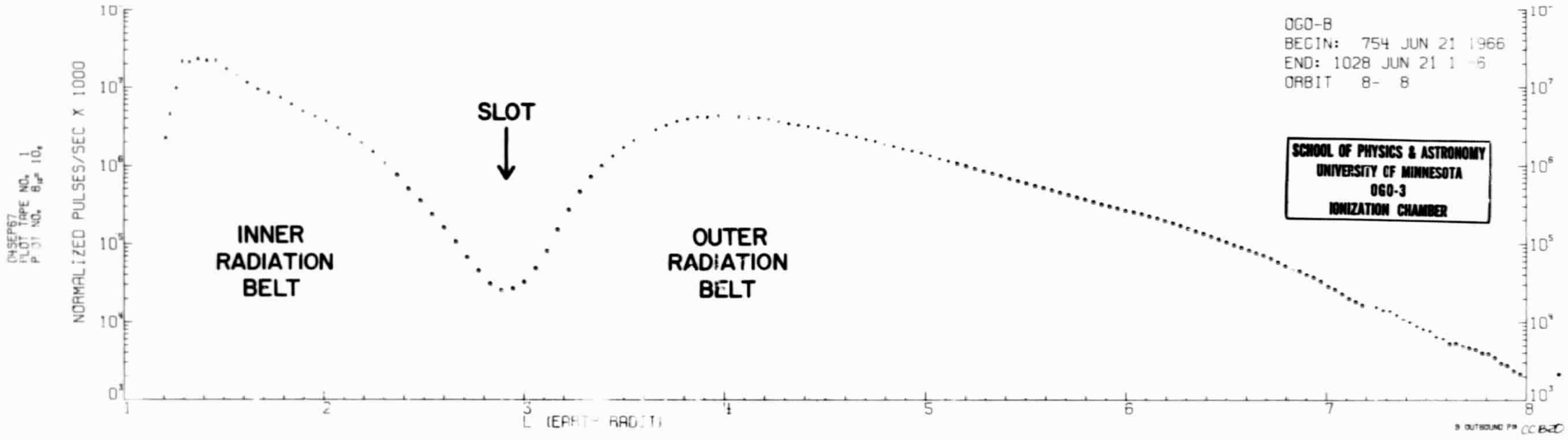

Figure 10

The radiation belt portion of Figure 9 plotted versus L. See Figure 6 for another example and a detailed description.

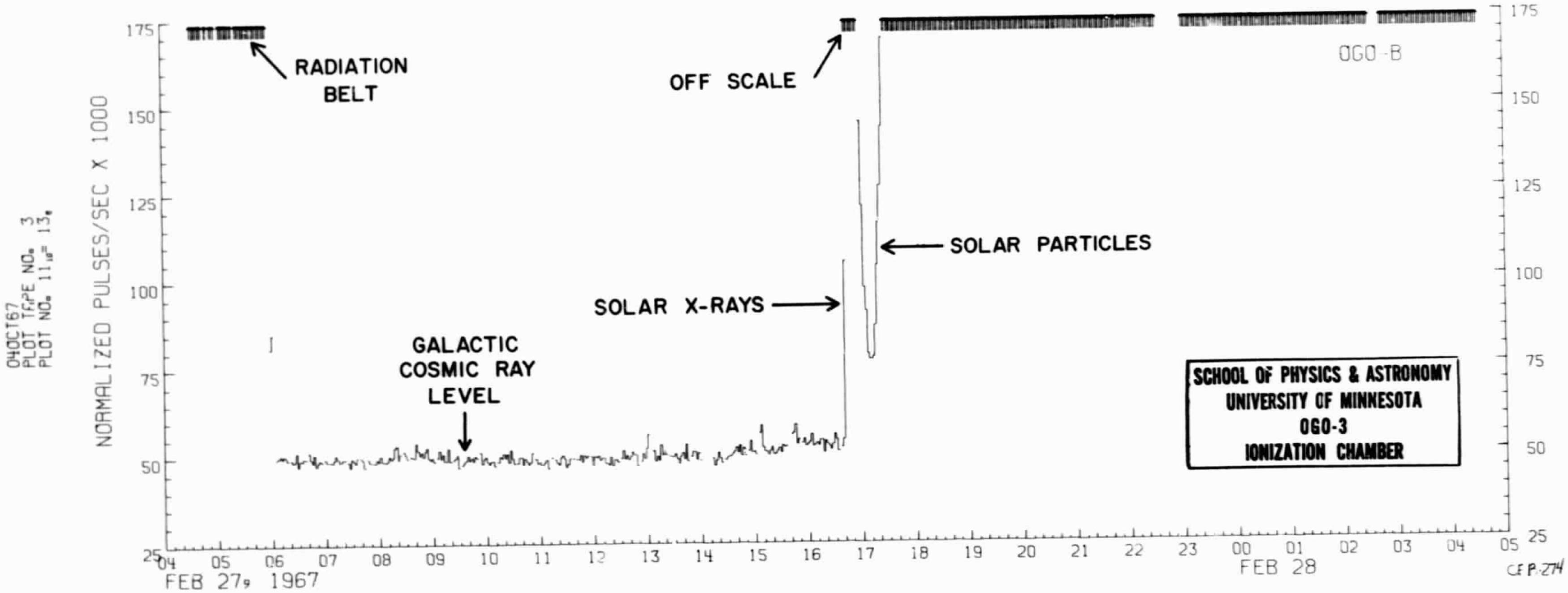

Figure 11

An example of an expanded time scale plot. One-minute averages are plotted on one-third of an orbit per plot. This particular figure shows a solar X-ray burst followed by a solar particle event observed outside the magnetosphere. The solar particles are thought to be protons (E > 12 meV), although an electron (E > 600 keV) contribution cannot positively be excluded.

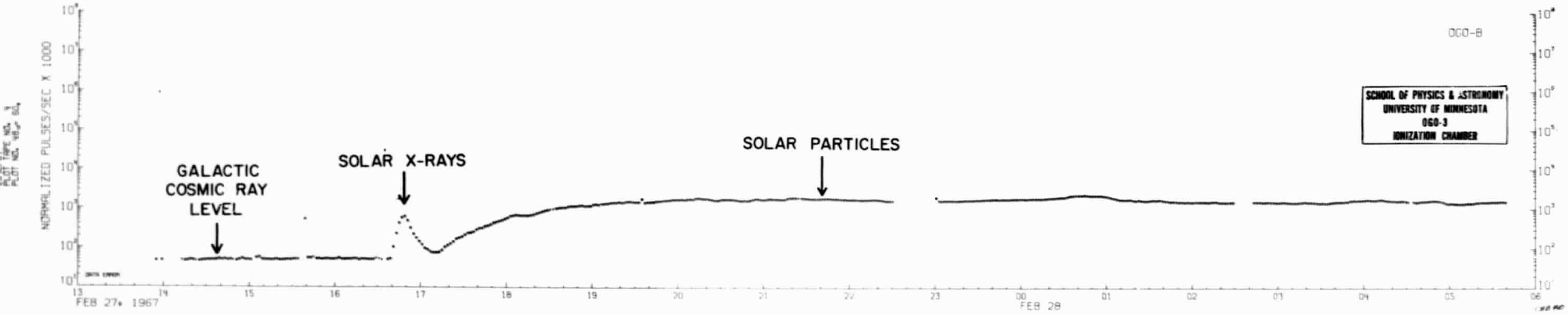

Figure 12

An expanded linear plot of 2 minute averaged chamber data used primarily for studying small fluctuations in the galactic cosmic rays. This plot covers the time covered by the previous plot and one can see that the X-ray burst as well as the solar proton event are off scale.

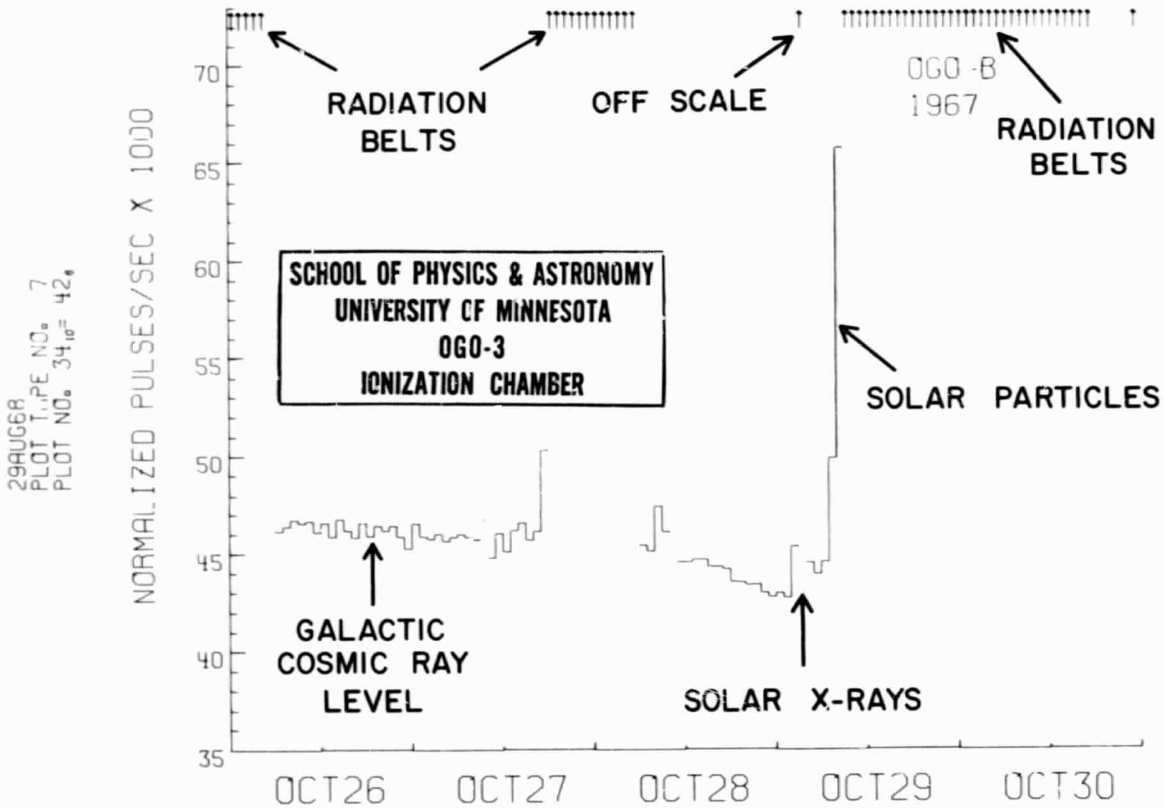

Figure 13

Hourly averages plotted on a five day per graph basis. These plots are used in the long term study of galactic cosmic rays.

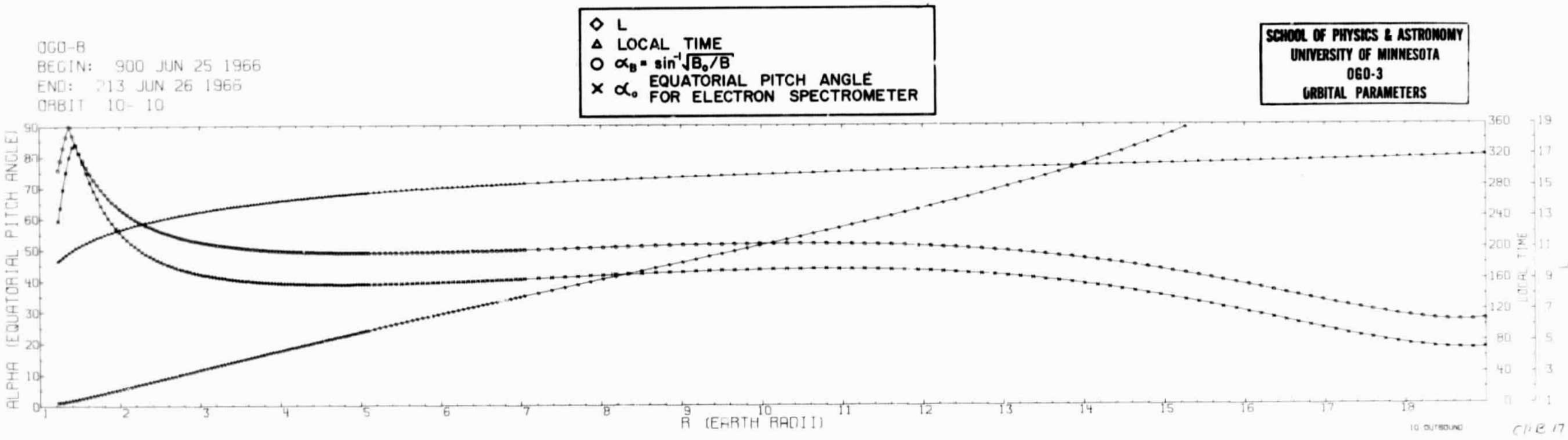

Figure 14

Orbital parameters are plotted vs. range to correspond to the data plots. The orbital plots are available only for orbits where either ion chamber or spectrometer data are available. The local time is expressed in degrees (0-360) with 0° corresponding to the midnight meridian. α_0 represents the spectrometer equatorial pitch angle whereas α_B represents the limiting look direction for the ion chamber (i.e. the ion chamber sees all particles whose equatorial pitch angle is less than α_B). These look angles are calculated from the ideal field, and are, of course, meaningless for large distances. The McIlwain L parameter is also valid only for small L.

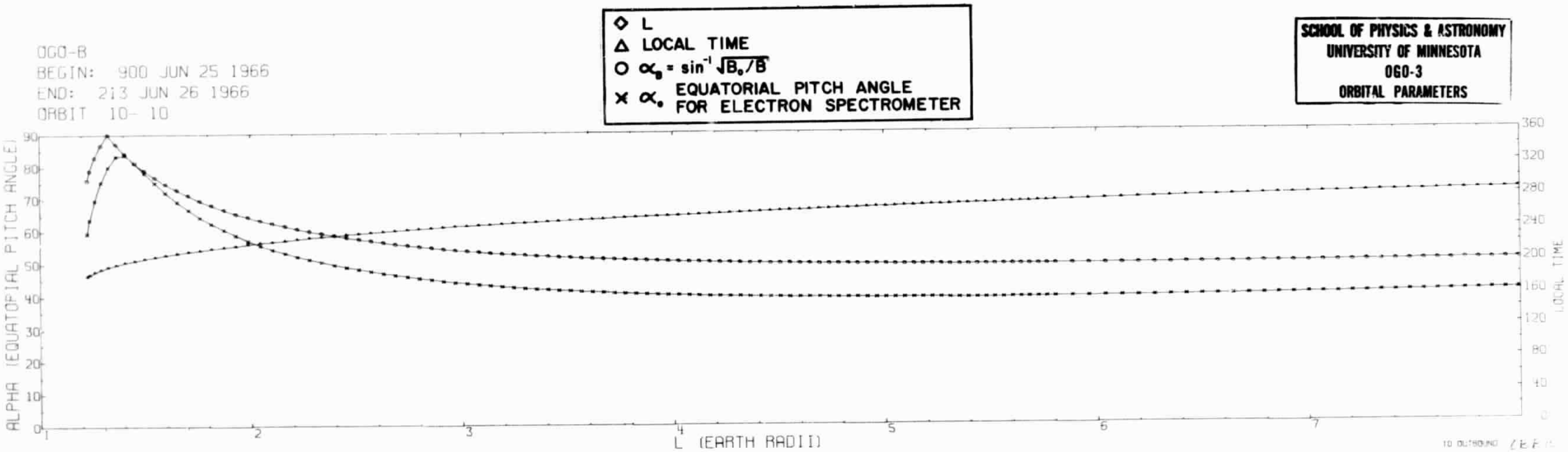

Figure 15

A plot of the orbital parameters versus the McIlwain L parameter corresponding to the L type data plots. See caption for Figure 14 for explanation of parameters.

III. Procedure for Computing Electron Flux and Energy Spectrums

All electron spectrometer data is plotted in an arbitrary scale which must be multiplied by a conversion factor to obtain the correct electron fluxes. The efficiencies of spectrometer channels I, II and III are quite independent of the incident electron spectrum; however, the efficiencies of channels IV and V are somewhat dependent on the incident electron spectrum.

If F_i is the arbitrary rate for channel i, as obtained from the plots, then

$$\frac{dJ_i}{dE} = A_i\ F_i \text{ electrons-cm}^{-2}\text{-sec}^{-1}\text{-ster}^{-1}\text{-keV}^{-1}$$

where dJ_i/dE is the differential directional electron flux and A_i is the conversion factor for channel i. A_i, the conversion factor, is spectrum dependent and is given by the expression

$$A_i = \frac{1}{g_i\ \bar{\varepsilon}_i\ \Delta E_i}$$

where g_i is an arbitrary constant, ΔE_i is the width of the energy channel and $\bar{\varepsilon}_i$ is the spectrum dependent efficiency factor.

The table below lists these constants for the case when the incident flux is a power spectrum of the form $dJ/dE = CE^{\gamma} = CE^{-3}$

Channel #	g_i	ΔE_i (keV)	$\bar{\varepsilon}_i$ ($\gamma = -3$)	A_i ($\gamma = -3$)
I	10000	70	1.8×10^{-7}	7.9
II	1300	170	6.2×10^{-7}	8.4
III	290	400	1.2×10^{-6}	7.2
IV	36	1010	2.9×10^{-6}	9.5
V	2.4	2300	1.2×10^{-5}	15.4

If, for example, the arbitrary rate for channel IV is $F_4 = 4 \times 10^2$, then $A_i = A_4 = 9.5$ (assuming $\gamma = -3$) from the above table, and we find that $dJ_4/dE = 38 \times 10^2$ electrons-cm^{-2}-sec^{-1}-ster^{-1}-keV^{-1}.

Using the conversion factors for the case of $\gamma = -3$ one obtains a reasonably accurate spectrum. If, however, the maximum accuracy is desired an iteration process must be used. For a more extensive treatment and for the necessary efficiency curves, the reader is referred to page 90-93 of Pfitzer, K. A., An Experimental Study of Electron Fluxes from 50 keV to 4 meV in the Inner Radiation Belt, Ph.D. Thesis, University of Minnesota Cosmic Ray Technical Report CR-123, August, 1968.

IV. Completed Data Plots Submitted to Data Center as of 31 December 1968

OGO-I Ion Chamber

Quantities Plotted: Time - Rate
Scale (X-Y): Linear - Log (symbols)

BEGIN DATE	END DATE	PLOT CODE	NO. OF PLOTS
9-12-64	12-31-64	CA-A-1 CA-A-41	41
2-11-65	6-19-65	CA-A-42 CA-A-85	44
8-9-65	12-7-65	CA-A-86 CA-A-127	42
12-15-66	5-27-66	CA-A-128 CA-A-171	44
9-2-66	12-11-66	CA-A-172 CA-A-209	38
3-3-67	6-5-67	CA-A-210 CA-A-244	35
			244 - Total

OGO-I Ion Chamber

Quantities Plotted: Time - Rate
Scale (X-Y): Linear - Log (histogram)

BEGIN DATE	END DATE	PLOT CODE	NO. OF PLOTS
9-7-64	1-1-65	CF-A-1 CF-A-44	44
2-8-65	6-21-65	CF-A-45 CF-A-92	48
8-8-65	12-20-65	CF-A-93 CF-A-140	48
1-5-66	5-28-66	CF-A-141 CF-A-187	47
8-30-66	12-11-66	CF-A-188 CF-A-226	39
3-3-67	6-5-67	CF-A-227 CF-A-262	36
			262 - Total

OGO-I Ion Chamber

Quantities Plotted: Geocentric distance (R) - Rate
Scale (X-Y): Linear - Log

BEGIN DATE	END DATE	PLOT CODE	NO. OF PLOTS
9-7-64	1-1-65	CD-A-1 CD-A-68	68
2-11-65	6-11-65	CD-A-69 CD-A-152	84
8-30-65	12-8-65	CD-A-153 CD-A-221	69
12-9-66	5-25-66	CD-A-222 CD-A-303	82
5-24-66	12-11-66	CD-A-304 CD-A-375	72
3-3-67	3-19-67	CD-A-376 CD-A-387	12
3-21-67	6-4-67	CD-A-388 CD-A-441	54
			441 - Total

OGO-I Ion Chamber

Quantities Plotted: L - Rate
Scale (X-Y): Linear - Log

BEGIN DATE	END DATE	PLOT CODE	NO. OF PLOTS
9-7-64	12-31-64	CC-A-1 CC-A-66	66
2-11-65	6-20-65	CC-A-67 CC-A-141	75
8-31-65	12-5-65	CC-A-142 CC-A-204	63
9-3-66	12-10-66	CC-A-205 CC-A-263	59
3-6-67	3-19-67	CC-A-264 CC-A-275	12
3-22-67	6-4-67	CC-A-276 CC-A-318	43
			318 - Total

OGO-I Ion Chamber

Quantities Plotted: Time - Rate
Scale (X-Y): Linear - Linear

BEGIN DATE	END DATE	PLOT CODE	NO. OF PLOTS
9-10-64	12-29-64	CE-A-1 CE-A-69	69
2-9-65	6-20-65	CE-A-70 CE-A-156	87
8-9-65	12-7-65	CE-A-157 CE-A-231	75
12-15-65	5-24-66	CE-A-232 CE-A-300	69
8-31-66	12-11-66	CE-A-301 CE-A-370	70
3-3-67	6-5-67	CE-A-371 CE-A-436	66
			436 - Total

OGO-I Ion Chamber

Quantities Plotted: Time - Rate (Inner Radiation Belt)
Scale (X-Y): Linear - Log (symbols)

BEGIN DATE	END DATE	PLOT CODE	NO. OF PLOTS
9-23-64	11-18-64	CB-A-1 CB-A-17	17
11-29-64	12-23-64	CB-A-18 CB-A-25	8
2-12-65	6-12-65	CB-A-26 CB-A-63	38
7-14-65	12-5-65	CB-A-64 CB-A-91	28
12-18-65	5-27-66	CB-A-92 CB-A-124	33
			124 - Total

OGO-I Electron Spectrometer

Quantities Plotted: Time - Rate (Inner Radiation Belt)
Scale (X-Y): Linear - Log

BEGIN DATE	END DATE	PLOT CODE	NO. OF PLOTS
9-15-64	12-23-64	EB-A-1 EB-A-25	25
2-12-65	6-20-65	EB-A-26 EB-A-64	39
9-2-65	12-5-65	EB-A-65 EB-A-91	27
2-17-66	5-27-66	EB-A-92 EB-A-117	26
			117 - Total

OGO-I Electron Spectrometer

Quantities Plotted: Time - Rate
Scale (X-Y): Linear - Log)

BEGIN DATE	END DATE	PLOT CODE	NO. OF PLOTS
9-7-64	12-31-64	EA-A-1 EA-A-41	41
2-11-65	6-19-65	EA-A-42 EA-A-83	42
8-9-65	8-17-65	EA-A-84 EA-A-86	3
9-2-65	12-15-65	EA-A-87 EA-A-121	35
2-17-66	5-27-66	EA-A-122 EA-A-158	37
9-2-66	12-10-66	EA-A-159 EA-A-196	38
3-3-67	6-4-67	EA-A-197 EA-A-230	34
			230 - Total

OGO-I Electron Spectrometer

Quantities Plotted: L - Rate
Scale (X-Y): Linear - Log

BEGIN DATE	END DATE	PLOT CODE	NO. OF PLOTS
9-7-64	12-31-64	EC-A-1-2 EC-A-65-66	65
2-11-65	6-20-65	EC-A-66-67 EC-A-143-144	78
9-2-65	12-5-65	EC-A-144-145 EC-A-202-203	59
9-3-66	12-8-66	EC-A-203-204 EC-A-261-262	59
3-3-67	6-4-67	EC-A-262-263 EC-A-312+9	51
			312 - Total

OGO-I Electron Spectrometer

Quantities Plotted: Geocentric Distance (R) - Rate
Scale (X-Y): Linear - Log

BEGIN DATE	END DATE	PLOT CODE	NO. OF PLOTS
9-7-64	12-31-64	ED-A-1 ED-A-68	68
2-11-65	6-12-65	ED-A-69 ED-A-151	83
9-1-65	1-11-66	ED-A-152 ED-A-220	69
2-16-66	5-25-66	ED-A-221 ED-A-285	65
8-31-66	12-11-66	ED-A-286 ED-A-354	69
3-3-67	3-19-67	ED-A-355 ED-A-365	11
3-20-67	6-4-67	ED-A-366 ED-A-409+8	52
			409 - Total

OGO-I Satellite Orbit

Quantities Plotted: L - Orbit parameters
Scale (X-Y): Linear - Linear

BEGIN DATE	END DATE	PLOT CODE	NO. OF PLOTS
9-7-64	12-31-64	DB-A-1 DB-A-69	69
2-11-65	6-20-65	DB-A-70 DB-A-151	82
8-31-65	12-5-65	DB-A-152 DB-A-215	64
9-2-66	12-10-66	DB-A-216 DB-A-279	64
3-3-67	3-19-67	DB-A-280 DB-A-292	13
3-22-67	6-4-67	DB-A-293 DB-A-340	48
			340 - Total

OGO-I Satellite Orbit

Quantities Plotted: Geocentric Distance (R) - Orbit Parameters
Scale (X-Y): Linear - Linear

BEGIN DATE	END DATE	PLOT CODE	NO. OF PLOTS
9-7-64	1-1-65	DA-A-1 DA-A-69	69
2-11-65	6-25-65	DA-A-70 DA-A-151	82
8-30-65	12-19-65	DA-A-152 DA-A-227	76
1-6-66	5-25-66	DA-A-228 DA-A-304	77
8-31-66	12-11-66	DA-A-305 DA-A-373	69
3-4-67	3-19-67	DA-A-374 DA-A-385	12
3-21-67	6-4-67	DA-A-386 DA-A-436	51
			436 - Total

OGO-III Ion Chamber

Quantities Plotted: Time - Rate
Scale (X-Y): Linear - Log (Histogram)

BEGIN DATE	END DATE	PLOT CODE	NO. OF PLOTS
6-9-66	7-23-66	CF-B-1 CF-B-44	44
7-24-66	7-23-67	CF-B-45 CF-B-225	180
7-25-67	10-1-67	CF-B-226 CF-B-259	33
			259 - Total

OGO-III Ion Chamber

Quantities Plotted: Time - Rate
Scale (X-Y): Linear - Log (Symbols)

BEGIN DATE	END DATE	PLOT CODE	NO. OF PLOTS
6-9-66	7-23-66	CA-B-1 CA-B-131	131
7-27-66	7-31-67	CA-B-132 CA-B-662	530
8-1-67	10-2-67	CA-B-663 CA-B-756	93
			756 - Total

OGO-III Ion Chamber

Quantities Plotted: Geocentric Distance(R) - Rate
Scale (X-Y): Linear - Log

BEGIN DATE	END DATE	PLOT CODE	NO. OF PLOTS
6-9-66	7-23-66	CD-B-1 CD-B-86	86
7-27-66	2-4-67	CD-B-87 CD-B-265	178
2-5-67	7-6-67	CD-B-266 CD-B-412	146
			412 - Total

OGO-III Ion Chamber

Quantities Plotted: L - Rate
Scale (X-Y): Linear - Log

BEGIN DATE	END DATE	PLOT CODE	NO. OF PLOTS
6-11-66	7-23-66	CC-B-1 CC-B-74	74
7-27-66	2-4-67	CC-B-75 CC-B-227	152
2-5-67	7-6-67	CC-B-228 CC-B-351	123
			351 - Total

OGO-III Ion Chamber

Quantities Plotted: Time - Rate
Scale (X-Y): Linear - Linear

BEGIN DATE	END DATE	PLOT CODE	NO. OF PLOTS
6-9-66	7-23-66	CE-B-1 CE-B-89	89
7-27-66	7-11-67	CE-B-90 CE-B-406	316
7-12-67	10-1-67	CE-B-407 CE-B-485	78
			485 - Total

OGO-III Ion Chamber

Quantities Plotted: Time - Rate (Inner Radiation Belt)
Scale (X-Y): Linear - Log (Histogram)

BEGIN DATE	END DATE	PLOT CODE	NO. OF PLOTS
6-11-66	7-23-66	CB-B-1 CB-B-35	35
7-27-66	7-4-67	CB-B-36 CB-B-189	153
7-6-67	10-1-67	CB-B-190 CB-B-231	41
			231 - Total

OGO-III Electron Spectrometer

Quantities Plotted: Time - Rate (Inner Radiation Belt)
Scale (X-Y): Linear - Log

BEGIN DATE	END DATE	PLOT CODE	NO. OF PLOTS
6-11-66	7-23-66	EB-B-1 EB-B-35	35
8-2-66	3-21-67	EB-B-36 EB-B-140	104
8-25-66	10-1-67	EB-B-141 EB-B-232	91
			232 - Total

OGO-III Electron Spectrometer

Quantities Plotted: Time - Rate
Scale (X-Y): Linear - Log

BEGIN DATE	END DATE	PLOT CODE	NO. OF PLOTS
6-9-66	7-23-66	EA-B-1 EA-B-232	232
8-2-66	4-1-68	EA-B-233 EA-B-516	283
4-4-67	6-28-67	EA-B-517 EA-B-596	79
6-30-67	7-31-67	EA-B-597 EA-B-625	28
8-1-67	10-2-67	EA-B-626 EA-B-686	60
			686 - Total

OGO-III Electron Spectrometer

Quantities Plotted: L - Rate
Scale (X-Y): Linear - Log

BEGIN DATE	END DATE	PLOT CODE	NO. OF PLOTS
6-11-66	7-23-66	EC-B-1 EC-B-73	73
8-2-66	2-4-67	EC-B-74 EC-B-230	156
2-6-67	7-4-67	EC-B-231 EC-B-343	112
			343 - Total

OGO-III Electron Spectrometer

Quantities Plotted: Geocentric Distance(R) - Rate
Scale (X-Y): Linear - Log

BEGIN DATE	END DATE	PLOT CODE	NO. OF PLOTS
6-9-66	7-23-66	ED-B-1 ED-B-88	88
8-2-66	2-4-67	ED-B-89 ED-B-265	176
2-6-67	7-6-67	ED-B-266 ED-B-296	30
			296 - Total

OGO-III Satellite Orbit

Quantities Plotted: L - Orbit Parameters
Scale (X-Y): Linear - Linear

BEGIN DATE	END DATE	PLOT CODE	NO. OF PLOTS
6-10-66	2-4-67	DB-B-1 DB-B-209	209
2-6-67	7-6-67	DB-B-210 DB-B-338	128
			338 - Total

OGO-III Satellite Orbit

Quantities Plotted: Geocentric Distance (R) - Orbit Parameters
Scale (X-Y): Linear - Linear

BEGIN DATE	END DATE	PLOT CODE	NO. OF PLOTS
6-9-66	2-4-67	DA-B-1 DA-B-224	224
2-6-67	7-6-67	DA-B-225 DA-B-371	146
			371 - Total